PRAMANA
— journal of
physics

Vol. 54, No. 2
February 2000
pp. 269–274

A comparison of the intensity contours of fringes due to multiple reflection and spatial hole burning in semiclassical theory of laser

RITA MONI BORAH and G D BARUAH
Department of Physics, Dibrugarh University, Dibrugarh 786 004, India

MS received 13 July 1999; revised 24 November 1999

Abstract. A comparison between spatial burning in the semiclassical theory of laser and the intensity contours of the fringes due to multiple reflections in a Fabry–Perot cavity is presented. The concept of spatial hole burning is also used in a quantum well system.

Keywords. Spatial hole burning.

PACS Nos 42.55 Ah; 42.55 Px

1. Introduction

The semiclassical theory of semiconductor laser noise considers the spontaneous emission fluctuations as the major noise sources. They have influence on gain in a number of ways. The phenomena like spectral hole burning [1], carrier heating [2] and spatial hole burning [3,4] are mainly responsible for gain suppression in a laser cavity. Of particular importance is the phenomenon of spatial hole burning which appears naturally in the semiclassical theory of laser [4]. This hole burning appears in the graph representing the normalized population difference versus axial co-ordinate along a laser axis. Though the hole burned by the field intensity for non-moving atoms are seen to wash, for rapidly moving atoms [5] the effect is inherently present as noise in laser oscillator and amplifiers. Recently an analogy of the spatial hole burning with quantum well structures [6] has been shown. It is attractive to consider the concept of hole burning to strained quantum well structures [7] where the cavity lengths are of the order of few hundreds of Angstrom only. In this communication we present an analogy between the phenomenon of spatial hole burning and the intensity contour of multiply reflected beam inside a Fabry–Perot cavity. The basic principle of spectral hole burning was indeed applied by Arnand [8] in the case of complicated structures like strained quantum wells. It was shown that constant-voltage driven laser diodes generate amplitude squeezed light.

2. The analogy

The normalized population difference in terms of the density matrix ρ_{aa} and ρ_{bb} is given by

$$\frac{\rho_{aa} - \rho_{bb}}{N(z,t)} = \frac{1}{1 + R/R_{\rm s}}, \tag{1}$$

where the term in the LHS is the population difference, $R_{\rm s}$ is the saturation parameter

$$R_{\rm s} = \frac{\gamma_a \gamma_b}{2\gamma_{ab}}$$

and R is the rate constant given by

$$R = 1/2 \left(\frac{\mathcal{P} E_n}{\hbar}\right)^2 |U_n|^2 \gamma^{-1} \mathcal{L}(w - v_n),$$

where

$$\mathcal{L} = \frac{\gamma^2}{\gamma^2 + (w - v_a)^2}.$$

γ_a, γ_b decay rates from the upper and lower states respectively and

$$\gamma_{ab} = 1/2(\gamma_a + \gamma_b).$$

For a rate constant R with $U_n^2(Z) = \sin^2 K_n z$ dependence we have

$$\frac{R}{R_{\rm s}} = I_n \left(\frac{2\gamma_{ab}}{\gamma}\right) \frac{\gamma^2}{\gamma^2 + (w - v_n)^2}, \tag{2}$$

where $I_n = 1/2(\mathcal{P}^2 E^2/\hbar^2 \gamma_a \gamma_b)$ is the dimensionless intensity $K_n = 2\pi/\lambda$. For central tuning $w - v_n = 0$ and using $\gamma = 2\gamma_{ab}$ eq. (1) becomes

$$\rho_{aa} - \rho_{bb} = \frac{N(z,t)}{1 + I_n \sin^2 K_a z}. \tag{3}$$

The normalized population difference versus axial co-ordinates Z is shown in figure 1. Spatial holes burned by the laser field in this difference for various value of dimensionless intensities $I_n = 0.25, 0.5, 1, 3$ and 1000 are depicted. We now consider the intensity contour of fringes due to multiple reflections inside a Fabry–Perot cavity. In this case the intensity of the transmitted rays may be worked out [9] as

$$I_T = \frac{\mathbf{I}_0}{1 + [4r^2/(1 - r^2)^2] \sin^2 \delta/2}, \tag{4}$$

where $\delta = 2\pi m$, at maxima $\sin^2(\delta/2) = 0$ and $\mathbf{I}_T = \mathbf{I}_0$, when the reflectance r^2 is large, approaching unity the quantity $4r^2/(1 - r^2)^2$ will also be large and even a small departure of δ from its values for maximum will result in a rapid drop of intensity. Figure 2 shows the intensity contour for $r = 0.235, 0.314, 0.415, 0.580$ and 0.9998. As may be inferred

from figures 1 and 2, dimensionless intensity corresponds to the reflectance as shown in table 1.

The case of decrease in the magnitude of the normalized population density with the increase in dimensionless intensity has its parallel in the intensity contour of fringes due to multiple reflections where it is shown that the sharpness of fringes or transmitted beam depends on reflectance.

Comparing eqs (2) and (3) we note that

$$\rho_{aa} - \rho_{bb} \equiv I_T, \quad I \equiv \frac{4r^2}{(1-r^2)^2}, \quad N(z,t) \equiv I_0$$

$$2\pi z/\lambda \equiv \delta \equiv 2\pi m.$$

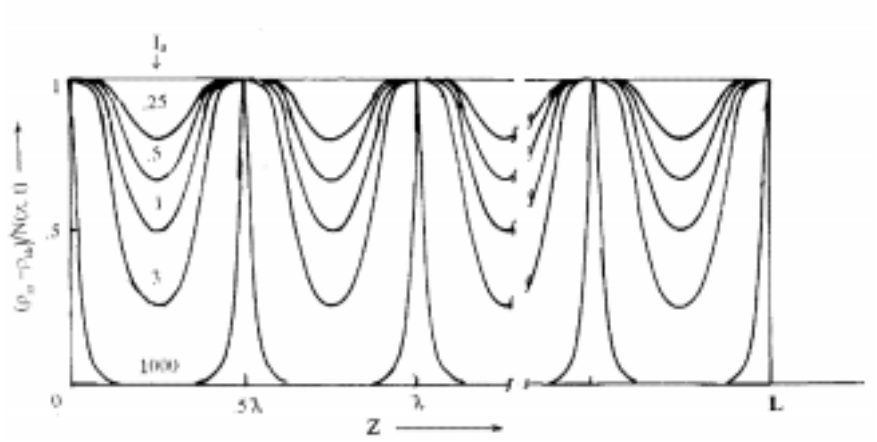

Figure 1. Normalized population difference versus axial coordinates. Spatial holes are burnt for various values of $\mathbf{I}_a$.

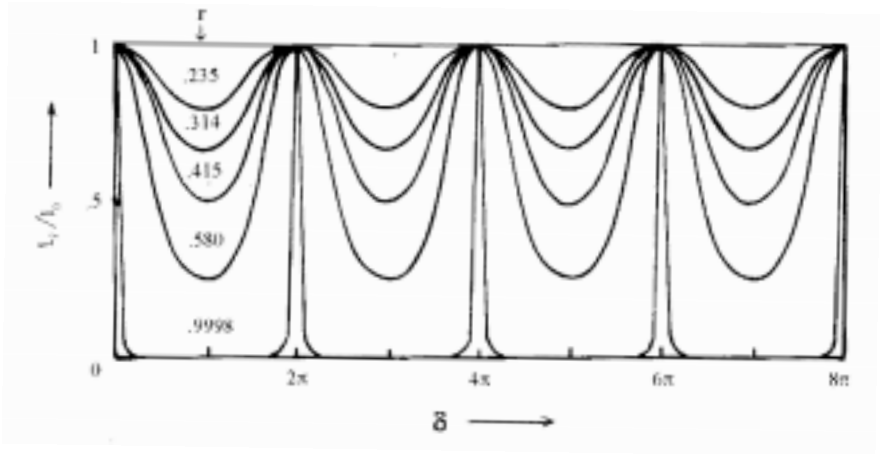

Figure 2. Intensity contour of fringes due to multiple reflections indicating exact analogy with spatial holes.

Table 1. A comparison between dimensionless intensity and reflectance.

Dimensionless intensity	Reflectance
0.25	0.235
0.5	0.314
1	0.415
3	0.580
1000	0.9998

We may also use a simple geometrical construction to find the resultant amplitude at different values of reflectance. We note that the amplitude of the transmitted rays are given by att^1, att^1r^2, $att^1r^4, \ldots$ or in general for the nth ray by att^1r^{2n}, where t and t^1 are the fraction of the transmitted ray intensities. In figure 3a the magnitudes of the amplitudes of first six transmitted rays are drawn for $r = 0.9998$. Starting at any principal maximum with $\delta = 2\pi m$, the individual amplitudes will be in phase with each other, so that the vectors are all drawn parallel to give a resultant.

If we now go slightly to one side of the maximum where the phase difference introduced between successive rays is $\pi/10$, each of the individual vectors must be drawn making an angle of $\pi/10$ with the preceding one and the resultant found by joining the tail of the first to the head of the last. Similar situations have been shown by introducing a phase difference of $\pi/5$ and $\pi/4$. Similar vector diagrams have been drawn for the magnitudes of the amplitudes of the first six transmitted rays for reflectances $r = 0.580$, 0.415, 0.314 and 0.235 with phases $\pi/10$, $\pi/5$, and $\pi/4$. They are shown in figures 3b–e respectively. It is worthwhile to note that similar vector representation for the dimensionless intensity 1000 is not possible but for the remaining values of dimensionless intensities 0.25, 0.5 and 1, we obtain only straight lines. For the dimensionless intensity of 3 the vector diagram is shown in figure 4.

From what has been described above it is reasonable to believe that we can use vectorial representation of dimensionless intensity in spatial hole burning to estimate the intensity of laser system. We observe that the number of holes inside a cavity also depends on the wavelength λ. As for example for a wavelength corresponding to the He–Ne laser 6328 Å, the number of spatial holes burnt inside a cavity of length 10 cm is 3.2×10^5. This also indicates the order of cavity modes. For a wavelength of 10^5 Å the number of holes will be 20,000. If the wavelength is 200 Å and the cavity length is 100 Å as in the case of a quantum well structure only one hole will appear. If the cavity length is 100 Å as in the case of quantum well structure and the wavelength is 100 Å the number of holes inside the cavity will be 2. This shows that the spatial hole burning is important when we consider cavity of dimensions of the order of few Angstrom only.

It is worthwhile to note that semiclassical theory is based on dipole approximation, which is also valid in quantum well system. The spatial holes in heterojunction lasers may play a dominant role in estimating the noise characteristics of the cavity. In the present work we have shown an exact analogy between the reflectance of the transmitted beam inside the F.P. cavity and the process of spatial hole burning. As indicated earlier for a reflectance nearing hundred per cent ($r = 0.9998$) the dimensionless intensity is 1000

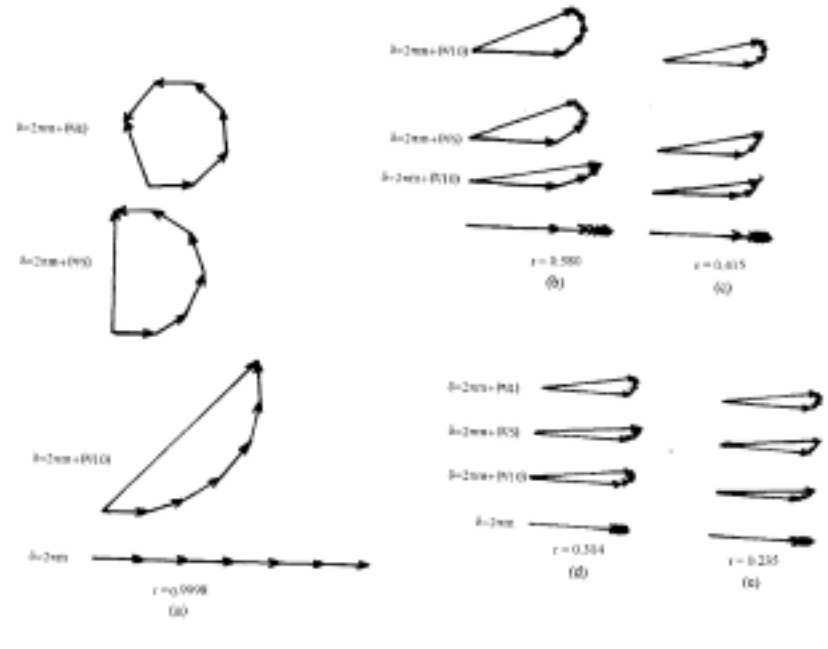

Figure 3. Geometrical construction representing the resultant amplitudes for six different values of reflectance.

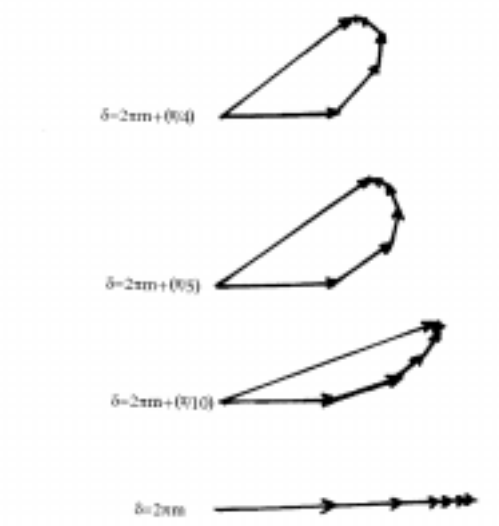

Figure 4. Geometrical construction of the resultant amplitude for dimensionless intensity 3.

which is prohibitably a large number. The value of dimensionless intensity is usually 1 for a typical He–Ne laser and the value usually does not exceed 30. At the same time hundred per cent reflectivity is an ideal case. For lower values the magnitude of the dimensionless intensity is equal to that of the reflectance. As for example for a value of dimensionless intensity 0.250 the reflectance is 0.235. The present analogy has been confined to single mode only. The multimode operation may modify the spatial hole burning pattern.

3. Conclusion

An analogy between spatial hole burning and the intensity contour of the beams in multiple reflection inside a Fabry–Perot cavity shows that the dimensionless intensity is identical to reflectance. There is a scope to use the concept to multiple quantum well structure.

References

[1] G P Agarwal and N K Dutta, *Long-wavelength semiclassical laser* (van Nostrand Reinhold, New York, 1986)
[2] X Plan, I I Olesen, B Tromborg and H E Lassen, *Proc. IEEE J.* **139**, 189 (1992)
[3] T Takahashi and Y Arakawa, *IEEE photon Jechnot. Lett.* **3**, 106 (1991)
[4] M Sargent III, M O Scully and W E Lamb, *Jr. Laser Physics* (Addison-Wesley, Reading Mass, 1974)
[5] S Stenholm and W E Lamb, *J. Phys. Rev.* **181**, 115 (1969)
[6] R Borah and G D Baruah, *Asian J. Chem.* **3**, 63 (1999)
[7] H C Casey Jr. and M P Paris, *Heterostructure laser* (Academic Inc., New York, 1978)
[8] J Arnaud, *Phys. Rev.* **A48**, 2235 (1993)
[9] F A Jenkins and H E White, *Fundamental of Optics* McGraw Hill International Edition (1981)